# Safe Planning in Interactive Environments via Iterative Policy Updates and Adversarially Robust Conformal Prediction

Omid Mirzaeedodangeh<sup>1</sup>, Eliot Shekhtman<sup>2</sup>, Nikolai Matni<sup>2,3</sup>, and Lars Lindemann<sup>1</sup>

<sup>1</sup>Automatic Control Laboratory, ETH Zürich, Switzerland <sup>2</sup>Computer and Information Science, University of Pennsylvania, USA <sup>2</sup>Electrical and Systems Engineering, University of Pennsylvania, USA

#### **Abstract**

Safe planning of an autonomous agent in interactive environments – such as the control of a selfdriving vehicle among pedestrians and human-controlled vehicles – poses a major challenge as the behavior of the environment is unknown and reactive to the behavior of the autonomous agent. This coupling gives rise to interaction-driven distribution shifts where the autonomous agent's control policy may change the environment's behavior, thereby invalidating safety guarantees in existing work. Indeed, recent works have used conformal prediction (CP) to generate distribution-free safety guarantees using observed data of the environment. However, CP's assumption on data exchangeability is violated in interactive settings due to a circular dependency where a control policy update changes the environment's behavior, and vice versa. To address this gap, we propose an iterative framework that robustly maintains safety guarantees across policy updates by quantifying the potential impact of a planned policy update on the environment's behavior. We realize this via adversarially robust CP where we perform a regular CP step in each episode using observed data under the current policy, but then transfer safety guarantees across policy updates by analytically adjusting the CP result to account for distribution shifts. This adjustment is performed based on a policy-to-trajectory sensitivity analysis, resulting in a safe, episodic open-loop planner. We further conduct a contraction analysis of the system providing conditions under which both the CP results and the policy updates are guaranteed to converge. We empirically demonstrate these safety and convergence guarantees on a two-dimensional car-pedestrian case study. To the best of our knowledge, these are the first results that provide valid safety guarantees in such interactive settings.

*Index terms*— Safe planning in interactive environments, distribution shifts, adversarially robust conformal prediction, iterative control policy updates.

# 1 Introduction

Autonomous agents, e.g., self-driving vehicles and service robots, are increasingly deployed in human-centric, multi-agent environments [1, 2]. The safe control of an autonomous agent is challenging as the behavior of uncontrollable agents, e.g., pedestrians, are unknown and interactive, i.e., they may react to the behavior of the autonomous agent. This creates an intricate coupling and interaction-driven distribution shift where the distribution of uncontrollable agent behaviors changes with the control policy of the autonomous agent. In this paper, we address this "chicken-and-egg" problem where changing the control policy changes the behavior of uncontrollable agents, and vice versa, see Figure 1.

Non-interactive approaches sequentially integrate predictions of uncontrollable agents into the design of the control policy [3, 4], while interactive approaches simultaneously predict uncontrollable agents and design control policies to take interactions directly into account [5, 6]. Non-interactive approaches usually assume worst-case interaction bounds to provide safety guarantees, therefore tending to be conservative. Interactive approaches perform better in practice, but fail to provide any safety guarantees. In this paper, we propose a planning framework that takes interaction into account and enjoys formal safety guarantees via iterative policy updates and robust conformal prediction.

Safe planning with conformal prediction. Conformal prediction (CP) is an uncertainty quantification technique that provides statistical guarantees for test data after a one-time calibration on held-out calibration data [7, 8]. CP has been used to construct prediction sets for uncontrollable agents that contain their true but unknown behavior with a user-specified probability [9, 10, 11]. These works learn a trajectory predictor (e.g., a recurrent neural network) for uncontrollable agents and perform calibration over

search [19], and LLM planning [20, 21], see [22] for a survey.

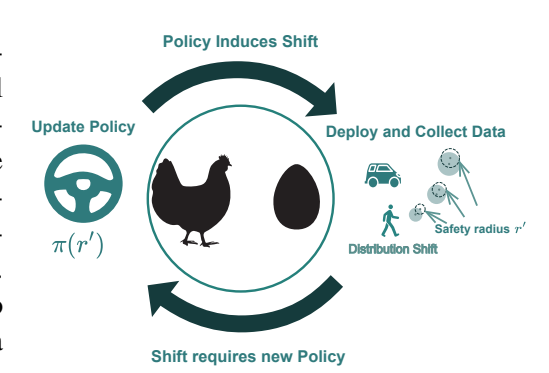


Figure 1: "Chicken-and-egg" problem: A change in policy can induce a distribution shift in the environment, here a pedestrian. This shift results in a modified safety radius r' that captures the pedestrian's behavior under this policy. This modified safety radius in turn requires a policy update  $\pi(r')$ . a nonconformity score that measures the deviation between the predicted and the true motion on held-out trajectories. The resulting calibration result defines a set around new predictions that is probabilistically valid and thereby operational, i.e., suitable for motion planning. This has been explored via model predictive control [12, 13, 14], reinforcement learning [15, 16], control barrier functions [17, 18], sampling-based

Interaction breaks conformal prediction guarantees. CP presumes that the data at test time is exchangeable with the data at calibration time. Indeed, simply using non-exchangeable calibration data can break conformal prediction guarantees, see e.g., [23, 24]. In interactive settings the premise of exchangeability is violated due to a circular dependency induced by interaction-driven distribution shifts: changing the control policy changes the data distribution at test time, while updating the held-out calibration data changes the control policy. Many CP extensions aim to mitigate this issue, e.g., via adaptive CP [25, 26], CP for covariate shifts [23, 27, 28], or robust CP [29, 30, 31]. However, these extensions either require continual recalibration or additional estimators, yield undersirable time-averaged or worst-case guarantees, or do not close the loop with a planner whose policy changes drive the distribution shift. Our interactive setting demands a mechanism that (i) directly addresses policy-induced distribution shifts, and (ii) closes the loop with the planner.

Positioning and differences to prior work on planning with CP. Prior work embeds calibrated CP sets into the planner by either assuming exchangeability [12, 32, 33] or by using adaptive CP [13, 15, 14, 19]. Conceptually closest to our work are [34] and [35], which also address agent interactions with CP. [35] discretize the joint agent space and use CP to capture state-dependent interaction in each cell. However, data requirements grow exponentially with the state dimension without addressing the aforementioned core circular dependency. [34] propose iterative policy updates similar to our method, but without providing episodic safety guarantees as we enable via adversarially robust CP. Additionally, [34] provide safety guarantees only after convergence, which is generally not guaranteed. In contrast, we provide: (i) episodic safety guarantees by analytically bounding the distribution shift, and (ii) explicit conditions on episodic convergence via a

<sup>&</sup>lt;sup>1</sup>We note that independent and identically distributed data is automatically also exchangeable.

contraction analysis.

### 2 Problem Formulation

We consider the state of an ego agent  $x_t \in \mathbb{R}^{d_x}$ , its control input  $u_t \in \mathbb{R}^{d_u}$ , and the state of uncontrollable agents'  $y_t \in \mathbb{R}^{d_y}$  at discrete times  $t = 0, \dots, T$ . Their coupled dynamics are

$$x_{t+1} = f_X(x_t, u_t) \tag{1a}$$

$$y_{t+1} = f_Y(y_t, x_t, u_t, \nu_t)$$
 (1b)

with exogenous noise  $\nu_t$ , which is a random variable that models the uncontrollable agents' intentions. The mapping  $(x_t, u_t) \mapsto f_Y(\cdot, x_t, u_t, \cdot)$  captures agent interaction. Here, safety is encoded by a safety function  $H(x_{0:T}, y_{0:T})$  and defined over the entire trajectories  $x_{0:T}$  and  $y_{0:T}$ . The system is considered safe if  $H(x_{0:T}, y_{0:T}) \leq 0$ . We assume that the system (1) is Lipschitz continuous.

**Assumption 1.** There exist Lipschitz constants  $L_{Xx}, L_{Xu}, L_{Yy}, L_{Yx}, L_{Yu} \ge 0$  such that

$$||f_X(x,u) - f_X(x',u')||_2 \le L_{Xx}||x - x'||_2 + L_{Xu}||u - u'||_2$$
  
$$||f_Y(y,x,u,\nu) - f_Y(y',x',u',\nu)||_2 \le L_{Yy}||y - y'||_2 + L_{Yx}||x - x'||_2 + L_{Yu}||u - u'||_2$$

for all  $x, x' \in \mathbb{R}^{d_x}$ ,  $u, u' \in \mathbb{R}^{d_u}$ , and  $y, y' \in \mathbb{R}^{d_y}$ .

**Running Example.** We use a running example of a self-driving vehicle and a pedestrian with states  $x_t$  and  $y_t$  (e.g., position, velocity) and controls  $u_t$  (e.g., acceleration, steering). The dynamics  $f_Y(y_t, x_t, u_t, \nu_t)$  capture interaction as the pedestrian's future position  $y_{t+1}$  depends on their own state  $y_t$ , the vehicle's states  $x_t$  and actions  $u_t$ , and their own intentions  $\nu_t$ . A common way to define H is as the maximum violation of a separation constraint over time, e.g.,  $H(x_{0:T}, y_{0:T}) := \max_{0 \le t \le T} \left\{ b_t - c(x_t, y_t) \right\} \le 0$ ) where  $c(x_t, y_t)$  represents a separation measure such as the distance between the vehicle's position and the pedestrian's position and  $b_t \ge 0$  is a safety margin.

#### 2.1 The Idealized Chance-Constrained Planning Problem

Our ideal (unfortunately unattainable) objective is to find a control policy  $u_{0:T-1}$  that minimizes a performance cost  $J(x_{0:T}, u_{0:T-1})$  while satisfying a probabilistic safety guarantee:

$$\min_{u_{0:T-1}} J(x_{0:T}, u_{0:T-1}) \quad \text{s.t.} \quad \begin{cases} \mathbb{P}\{H(x_{0:T}, y_{0:T}) \le 0\} \ge 1 - \alpha \\ \text{Dynamics in equation (1)} \end{cases} \tag{2}$$

The problem (2) is generally intractable. First, the uncontrollable agents' dynamics  $f_Y$  and the noise distribution of  $\nu_t$  are typically unknown, e.g., we cannot precisely model interaction and intentions, requiring a model- and distribution-free approach. Second, the high-dimensionality of the problem induces computational complexity: even if  $f_Y$  and  $\nu_t$  were known, the chance constraint (2) would require solving a complex, high-dimensional integral over the distribution of  $y_{0:T}$ .

While the first two challenges have been addressed in the literature, the third and most difficult challenge arises due to **interaction-induced distribution shifts**. Effectively, the dynamics  $f_Y$  and the distribution of  $y_{0:T}$  are policy-dependent, meaning they change when the ego-agent's states  $x_t$  and control inputs  $u_t$  change, e.g., if the car accelerates aggressively, the pedestrian's decision to cross an intersection will change. Robust

control, which enforces safety for all permissible trajectories, is overly conservative. Statistical uncertainty quantification techniques – such as in [12] which use conformal prediction (CP) – fail as the policy-driven distribution shift breaks exchangeability assumptions needed in CP, e.g., data of a pedestrian crossing in front of a slow car is not exchangeable with the new scenario where the car accelerates. Our goal is hence to obtain guarantees that are both distribution-free and can be carried across policy updates.

### 2.2 Non-Interactive Planning with Distribution-Free Certificates via Conformal Prediction

We now summarize existing work on non-interactive planning – primarily following [12] – in which case  $f_Y$  does not depend on  $x_t$  and  $u_t$ , i.e., not addressing the third of the aforementioned challenges. These techniques will serve as a starting point for our proposed method.

First, a pre-designed offline predictor is used to produce a single, nominal estimate  $\hat{y}_{0:T} = (\hat{y}_0, \dots, \hat{y}_T)$  of the environment trajectory  $y_{0:T} = (y_0, \dots, y_T)$ . To assess the accuracy of this estimate, we define the nonconformity score and the induced trajectory tube, respectively, as

$$s(\hat{y}_{0:T}, y_{0:T}) := \max_{0 \le t \le T} \|\hat{y}_t - y_t\|_2, \tag{3a}$$

$$C_r(\hat{y}_{0:T}) := \{ y_{0:T} : s(\hat{y}_{0:T}, y_{0:T}) \le r \}.$$
(3b)

The threshold  $r \geq 0$  is computed using CP to obtain probabilistic guarantees on the correctness of the set  $\mathcal{C}_r(\hat{y}_{0:T})$ . The main idea is simple: we use a set of N held-out calibration trajectories  $\{y_{0:T}^{(i)}\}_{i=1}^N$  generated by the non-interactive dynamics  $y_{t+1}^{(i)} = f_Y(y_t^{(i)}, \nu_t^{(i)})$ . We then compute r as the  $(1-\alpha)$ -quantile of the held-out nonconformity scores, denoted by  $q_{1-\alpha}(\{s(\hat{y}_{0:T}, y_{0:T}^{(i)})\}_{i=1}^N)$ . Since the test trajectory  $y_{0:T}$  and the held-out trajectories  $\{y_{0:T}^{(i)}\}_{i=1}^N$  are exchangeable, we have that

$$\mathbb{P}_{N+1}\left\{y_{0:T} \in \mathcal{C}_{q_{1-\alpha}}(\hat{y}_{0:T})\right\} \geq 1 - \alpha,$$

where now  $\mathbb{P}_{N+1}\{\cdot\}$  is a product probability measure that captures the randomness in test  $y_{0:T}$  and calibration data  $\{y_{0:T}^{(i)}\}_{i=1}^N$ , and as such can approximate the chance constraint in equation (2). This guarantee motivates the formulation of the following robust planning problem:

$$\min_{u_{0:T-1}} J(x_{0:T}, u_{0:T-1})$$
(4a)

s.t. 
$$x_{t+1} = f_X(x_t, u_t), \quad t = 0, \dots, T - 1,$$
 (4b)

$$H(x_{0:T}, \zeta) \le 0 \quad \forall \zeta \in \mathcal{C}_{q_{1-\alpha}}(\hat{y}_{0:T}),$$
 (4c)

which ensures  $\mathbb{P}_{N+1}\{H(x_{0:T},y_{0:T})\leq 0\}\geq 1-\alpha$  in the non-interactive case whenever (4c) is feasible [12]. For instance, for the collision avoidance-type safety constraints  $H(x_{0:T},y_{0:T})=\max_{0\leq t\leq T}\{b_t-c(x_t,y_t)\}$ , the constraint (4c) reduces to a step-wise tightening of the form  $c(x_t,\hat{y}_t)\geq b_t+q_{1-\alpha}$  for all times  $t=0,\ldots,T$ , which can easily be implemented.

However, in the interactive case where the coupled agent dynamics are  $y_{t+1} = f_Y(y_t, x_t, u_t, \nu_t)$  instead of  $y_{t+1} = f_Y(y_t, \nu_t)$ , a circular dependency – or "chicken-and-egg" problem – emerges. Changing the control inputs  $u_t$  and ego-agent trajectory  $x_t$  changes the distribution of  $y_{0:T}$ , violating the exchangeability assumption with the held-out trajectories  $\{y_{0:T}^{(i)}\}_{i=1}^N$ . On the other hand, updating the held-out trajectories

<sup>&</sup>lt;sup>2</sup>The empirical quantile  $q_{1-\alpha}$  is computed from the set of scores  $\{s_i\}_{i=1}^N$ . Let  $s_{(k)}$  be the k-th smallest score (the k-th order statistic). Then, the quantile is  $q_{1-\alpha} = s_{(k)}$  with  $k = \lceil (N+1)(1-\alpha) \rceil$ .

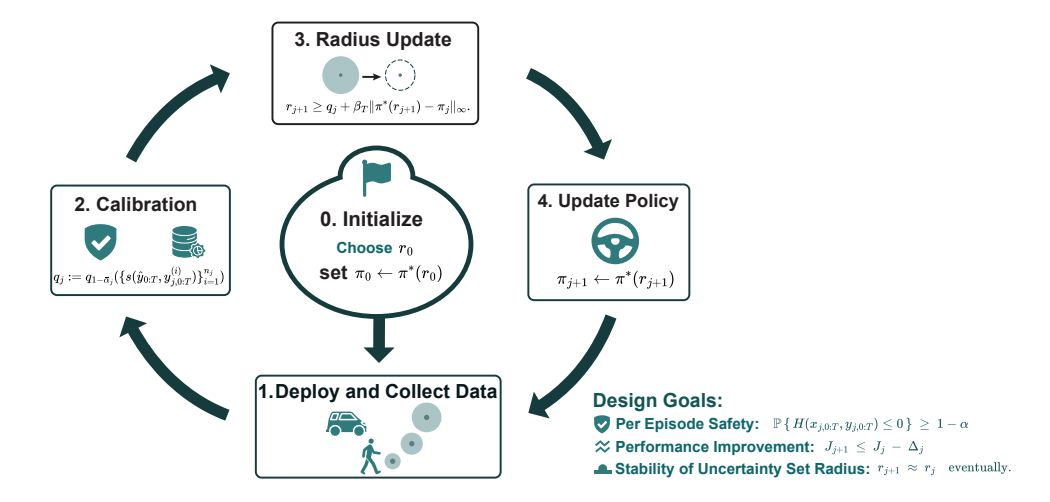


Figure 2: Our iterative algorithm consists of the following steps: (0) initialization via a safe (potentially conservative) radius  $r_0$  from which we compute a safe policy  $\pi^*(r_0)$ , (1) deploy policy  $\pi^*(r_j)$  and collect environment data under this policy, (2) calibrate prediction uncertainty  $q_j$  using the collected data, (3) compute new radius  $r_{j+1}$  from  $q_j$ , (4) update policy to  $\pi^*(r_{j+1})$ , and (5) rinse and repeat starting from step (1).

 $\{y_{0:T}^{(i)}\}_{i=1}^N$  via  $y_{t+1}^{(i)} = f_Y(y_t^{(i)}, x_t, u_t, \nu_t^{(i)})$ , changes the quantile  $q_{1-\alpha}$  and thereby  $u_t$  and  $x_t$ . To address this issue, we propose an episodic framework in which we iteratively compute new held-out trajectories while updating the control inputs.

Running Example (cont.). In our running example this non-interactive approach would first predict a nominal path  $\hat{y}_{0:T}$  for the pedestrian (e.g., walking straight on the sidewalk). The trajectory tube  $\mathcal{C}_r$  represents a tube of radius  $r=q_{1-\alpha}$  around this nominal path that guarantees the actual pedestrian path  $y_{0:T}$  will be inside this tube with  $1-\alpha$  probability, assuming the car's actions do not influence the pedestrian. The "chicken-and-egg" problem arises in the interactive case: the car's plan  $u_t$  depends on the size of the pedestrian's uncertainty set (the radius  $q_{1-\alpha}$ ), but the pedestrian's actual behavior, which determines the size of that tube, depends on the car's plan  $u_t$ .

#### 2.3 Episodic Problem Formulation and Design Goals

To address the aforementioned circular dependency, we reframe the problem into an iterative, episodic framework which we explain below and summarize in Figure 2. Planning proceeds in episodes  $j=0,1,2,\ldots$  We use a fixed nominal predictor  $\hat{y}_{0:T}=(\hat{y}_0,\ldots,\hat{y}_T)$  to anchor the geometry of the uncertainty. Updating the predictor episodically is possible with minimal modifications, but omitted here for simplicity. At each episode j, we solve the following robust optimization problem, parameterized by an uncertainty radius  $r_j \geq 0$ :

$$\mathbf{P}[j; r_{j}] \quad \min_{u_{j,0:T-1}} \quad J(x_{j,0:T}, u_{j,0:T-1}) \\
\text{s.t.} \quad x_{j,t+1} = f_{X}(x_{j,t}, u_{j,t}), \quad t = 0, \dots, T-1, \\
\quad H(x_{j,0:T}, \zeta) \leq 0 \quad \forall \zeta \in C_{r_{j}}(\hat{y}_{0:T}).$$
(5)

Solving (5) yields the policy  $\pi_j := u_{j,0:T-1}$  and the resulting optimal cost  $J_j := J(x_{j,0:T}, u_{j,0:T-1})$ . This policy is then executed on the physical system  $n_j$  times, which produces  $n_j$  i.i.d. rollouts of the environment's trajectories  $\left\{y_{j,0:T}^{(i)}\right\}_{i=1}^{n_j} \sim \mathcal{D}(\pi_j)$  under the ego-agent's policy, as governed by (1) and denoted by  $\mathcal{D}(\pi_i)$ . The design of this iterative process is driven by three high-level objectives:

**Per-episode safety:** 
$$\mathbb{P}\left\{H(x_{i,0:T}, y_{i,0:T}) \leq 0\right\} \geq 1 - \alpha \text{ for all } j,$$
 (6)

**Performance improvement:** 
$$J_{j+1} \leq J_j - \Delta_j \quad \text{with } \Delta_j \geq 0,$$
 (7) **Stability of uncertainty:**  $r_{j+1} \approx r_j \quad \text{eventually.}$  (8)

**Stability of uncertainty:** 
$$r_{i+1} \approx r_i$$
 eventually. (8)

The key challenge is to determine how to update  $r_j$  to  $r_{j+1}$ . This update must leverage the new data  $\{y_{i,0:T}^{(i)}\}$  to reduce conservatism, while also guaranteeing that the next policy  $\pi_{j+1}$  will be safe. Because  $r_j$ is implicitly tied to the policy  $\pi_i$  through interaction, the policy-induced distribution shift from j to j+1must be accounted for to maintain (6). We make the following assumption.

**Assumption 2.** At iteration 
$$j=0$$
, we know  $r_0$  s.t.  $\pi_0$  satisfies  $\mathbb{P}\left\{H(x_{0,0:T},y_{0,0:T})\leq 0\right\}\geq 1-\alpha$ .

This assumption is natural to our problem formulation. In practice, we can typically find this constant by selecting a sufficiently large  $r_0$  that is valid for any permissible ego agent policy.

**Running Example (cont.).** In episode j=0, assume that we have selected a valid uncertainty radius  $r_0$  for the ego agent's policy  $\pi_0$ , e.g., that the pedestrian will deviate at most  $r_0 = 2$  meters from its predicted path under  $\pi_0$  with probability of at least  $1-\alpha$ . We then observe realized pedestrian trajectories  $\{y_{0,0:T}^{(i)}\}$ under  $\pi_0$ , where we may now notice that the pedestrian may deviate less than  $r_0$  meters from the predicted path. The key challenge is hence to iteratively update the next radii  $r_1, r_2, \ldots$  and compute the next policies  $\pi_1, \pi_2$  while adhering to the objectives in (6)-(8).

#### 3 An Iterative Planning Framework for Interactive Environments

In our interactive setting, the exchangeability assumption underlying CP is violated at every policy update. When we solve (5) and update the policy from  $\pi_i$  to  $\pi_{i+1}$ , the realized trajectory  $y_{i+1,0:T}$  is drawn from a different distribution. This re-introduces the "chicken-and-egg" problem.

## **Adversarial Conformal Prediction for Policy-Induced Shifts**

To carry safety certificates across such policy-induced shifts, our approach uses adversarial conformal prediction (ACP), which provides guarantees under bounded perturbations [31]. Let  $z \sim \mathcal{D}$  be a random variable and  $\hat{z}$  be an estimate of z. Given a nonconformity score  $s(\hat{z},z)$  and an adversarial budget  $\rho \geq 0$ , ACP provides coverage for  $s(\hat{z}, z + \Delta)$  where the random variable z may be perturbed by any  $\Delta$  with  $\|\Delta\| \le \rho$ . The next result follows by combining ACP with conditional CP [36], which is also summarized in [22, Lemma 2].

**Lemma 1** ([31] and [36]). Let  $z, z^{(1)}, \ldots, z^{(N)} \sim \mathcal{D}$  be exchangeable random variables,  $\rho > 0$  be an adversarial budget,  $\alpha, \delta \in (0,1)$  be failure probabilities, and

$$r = q_{1-\bar{\alpha}}(\{s(\hat{z}, z^{(i)})\}_{i=1}^{N})$$

be the inflated  $(1-\bar{\alpha})$ -quantile of the unperturbed nonconformity scores  $\{s(\hat{z},z^{(i)})\}_{i=1}^N$  where  $\bar{\alpha}:=\alpha-1$  $\sqrt{\ln(1/\delta)/2N}$ . Assume there exists a constant  $M \geq 0$  such that for all z it holds that  $\sup_{\|\Delta\| \leq \rho} s(\hat{z}, z + z)$   $\Delta$ )  $\leq s(\hat{z},z) + M.^3$  Then, we have that

$$\mathbb{P}_{N}\left\{ \mathbb{P}\left\{ \forall \Delta \text{ with } \|\Delta\| \leq \rho : \ z + \Delta \in \mathcal{C}_{r}^{adv}(\hat{z}; \rho) \right\} \geq 1 - \alpha \right\} \geq 1 - \delta. \tag{9}$$

where  $C_r^{adv}(\hat{z};\rho) := \{z : s(\hat{z},z) \le r + M\}$  is an inflated prediction set.

We note that the guarantees in (9) are conditional in the sense that  $\mathbb{P}_N\{\cdot\}$  is a product probability measure that captures randomness in the calibration data  $\{z^{(i)}\}_{i=1}^N$ , so that the inner probability measure  $\mathbb{P}\{\cdot\}$  captures randomness over test data z that holds with probability no less than  $1-\delta$ .

To address the "chicken-and-egg" problem, we will apply robustification via ACP iteratively. At each episode j, we perform a recalibration step using the new data  $\{y_{j,0:T}^{(i)}\}_{i=1}^{n_j} \sim \mathcal{D}(\pi_j)$  to compute the latest inflated empirical  $(1-\bar{\alpha}_j)$ -quantile

$$q_j := q_{1-\bar{\alpha}_j}(\{s(\hat{y}_{0:T}, y_{j,0:T}^{(i)})\}_{i=1}^{n_j})$$

where  $\bar{\alpha}_j := \alpha - \sqrt{\ln(1/\delta)/2n_j}$ . By Lemma 1, this empirical quantile  $q_j$  satisfies  $\mathbb{P}_{n_j} \big\{ \mathbb{P} \big\{ y_{j,0:T} \in \mathcal{C}_{q_j}(\hat{y}_{0:T}) \big\} \geq 1 - \alpha \big\} \geq 1 - \delta$ , where  $y_{j,0:T} \sim \mathcal{D}(\pi_j)$  and  $\mathcal{C}_{q_j}(\hat{y}_{0:T}) := \{y_{0:T} : s(\hat{y}_{0:T}, y_{0:T}) \leq q_j \}$ . Thus,  $q_j$  is a valid safety radius for policy  $\pi_j$ . To maintain safety for the next policy  $\pi_{j+1}$ , we must now account for policy-induced distribution shifts caused by the change from  $\pi_j$  to  $\pi_{j+1}$ . We interpret and treat the policy update from  $\pi_j$  to  $\pi_{j+1}$  as the adversarial perturbation term  $\rho_j$ .

**High-level intuition.** Let us provide some intuition before we present the iterative algorithm and a detailed analysis in Sections 3.2 and 3.3, respectively. Under Assumption 1, we can bound the change in the uncontrollable agents trajectory by a constant  $\beta_T \geq 0$  such that

$$\max_{0 \le t \le T} \|y_t(\pi_{j+1}) - y_t(\pi_j)\|_2 \le \beta_T \|\pi_{j+1} - \pi_j\|_{\infty},$$

where  $\|\pi_{j+1} - \pi_j\|_{\infty} := \max_{0 \le t \le T-1} \|u_{j+1,t} - u_{j,t}\|_2$ . We formalize the existence of  $\beta_T$  next and provide the proof in Appendix C.1.

**Lemma 2** (Episode Coupling Sensitivity). Let the system in equation (1) be given and Assumption 1 hold. Then there exists a constant  $\beta_T \geq 0$  which depends on the horizon T and the Lipschitz constants  $L_{Xx}, L_{Xu}, L_{Yy}, L_{Yx}, L_{Yu}$  such that for two policies  $\pi = \{u_t\}_{t=1}^{T-1}$  and  $\pi' = \{u'_t\}_{t=1}^{T-1}$ :

$$||y_{0:T}(\pi') - y_{0:T}(\pi)||_{\infty} \le \beta_T ||\pi' - \pi||_{\infty}$$

Next, note that our nonconformity score in equation (3) is 1-Lipschitz continuous. Therefore, we have

$$|s(\hat{y}_{0:T}, y_{j,0:T}) - s(\hat{y}_{0:T}, y_{j+1,0:T})| \le \beta_T \|\pi_{j+1} - \pi_j\|_{\infty}$$

so that the policy change can increase the nonconformity score by at most  $M_{j+1} := \beta_T \|\pi_{j+1} - \pi_j\|_{\infty}$ .

Using Lemma 1 and combining this term with the empirical quantile  $q_j$  yields a high-probability upper bound on the required radius for the next policy  $\pi_{j+1}$  that is of the form:

$$\mathbb{P}_{n_j} \left\{ \mathbb{P} \left\{ s(\hat{y}_{0:T}, y_{j+1,0:T}) \le q_j + M_{j+1} \right\} \ge 1 - \alpha \right\} \ge 1 - \delta.$$
 (10)

This motivates our safe radius update rule  $r_{j+1} := q_j + M_{j+1}$  which is constructed to be a high-probability

<sup>&</sup>lt;sup>3</sup>If the nonconformity score s is Lipschitz continuous in its second argument with constant L, then  $M = L\rho$ .

<sup>&</sup>lt;sup>4</sup>We use the notation of  $y_t(\pi_j)$  instead of  $y_{j,t}$  to highlight that the trajectory  $y_t$  is a function of  $\pi_j$ .

upper bound on the true, unknown  $(1-\alpha)$ -quantile of the next distribution  $\mathcal{D}(\pi_{j+1})$ . Before deploying  $\pi_{j+1}$ , we solve the next planning problem  $P[j+1;r_{j+1}]$  using  $r_{j+1}$  as the required safety tube radius. By construction, any policy that is feasible for  $P[j+1;r_{j+1}]$  is guaranteed, with high probability, to remain safe against all environment trajectories in that inflated tube.

#### 3.2 The Iterative Planning Algorithm

We follow the previously described "recalibrate each episode, then transfer" approach. Algorithmically, the central challenge is to compute the next radius  $r_{j+1}$ , which must ensure safety for the next policy  $\pi_{j+1}$  before we have even computed  $\pi_{j+1}$ . Formally, to compute  $\pi_{j+1}$  we need to know  $r_{j+1}$  for which we have to know  $M_{j+1}$ , which in turn depends on  $\pi_{j+1}$ , creating an implicit problem. We first define this problem and then present two ways to solve it: a computationally expensive but exact "implicit solver" and a computationally cheap "explicit solution" (used in our main analysis).

**Implicit Safety.** From equation (10),  $r_{j+1}$  must cover  $q_j$  and the policy-induced shift  $M_{j+1}$  such that  $r_{j+1} \ge q_j + M_{j+1}$ . However, the policy-shift budget  $M_{j+1}$  depends on the policy  $\pi_{j+1}$  that we are trying to find, since  $\pi_{j+1} = \pi^*(r_{j+1})$ . This gives the true, implicit safety requirement:

$$r_{j+1} \ge q_j + \beta_T \|\pi^*(r_{j+1}) - \pi_j\|_{\infty}$$
 (11)

We are now looking for the smallest  $r_{j+1} \in \mathcal{R} := [r_{\min}, r_{\max}]$  that satisfies this inequality. We next present details for both solutions, which are summarized in Algorithm 1 in Appendix A.

Approach 1: The Implicit Solver (via Internal Iteration). We can solve the implicit inequality (11) directly using a numerical solver, such as a bisection search. This implicit algorithm treats the planner  $\pi^*(\cdot)$  as a black-box function. Our goal is to find the smallest  $r \in [q_j, r_{\max}]$  such that  $r \geq f(r)$ , where  $f(r) = q_j + \beta_T \|\pi^*(r) - \pi_j\|_{\infty}$ . We describe such a bisection procedure in Appendix B. Such a method is precise and finds the least conservative radius, but it is computationally very expensive, requiring many calls to the planner  $\pi^*(\cdot)$  within a single episode update.

Approach 2: The Tractable Explicit Solver. We here solve the implicit inequality (11) analytically. To get such an analytical bound, we assume that there exists a Lipschitz constant  $L_U \geq 0$  that bounds how much the optimal policy  $\pi^*(r)$  changes in response to a change in the radius  $r \in \mathcal{R}$ .

**Assumption 3.** There exists a Lipschitz constant  $L_U$  such that within an interval

$$\|\pi^*(r) - \pi^*(r')\|_{\infty} \le L_U |r - r'| \quad \forall r, r' \in \mathcal{R}.$$

The Lipschitz continuity property in Assumption 3 holds for many optimization-based planners. We provide a detailed analysis in Appendix C.2 for the common case in which the optimization problem P[j;r] is feasible, convex, and has a unique, regular optimizer. From here, we now get

$$\beta_T \|\pi^*(r_{j+1}) - \pi_j\|_{\infty} = \beta_T \|\pi^*(r_{j+1}) - \pi^*(r_j)\|_{\infty} \le \beta_T L_U |r_{j+1} - r_j| = \kappa |r_{j+1} - r_j|,$$

where  $\kappa := \beta_T L_U$  is a closed-loop gain that will help us analyze properties of our iterative planner. Instead of the implicit inequality (11), we can use this upper bound to get the sufficient inequality:

$$r_{j+1} \ge q_j + \kappa |r_{j+1} - r_j|$$
 (12)

The inequality (12) is a simple scalar inequality for  $r_{j+1}$ . As we will show in Section 3.3, this inequality has a unique, minimal (least conservative) solution, which is given by a closed-form expression. This is the

algorithm we use in our analysis in the next section. It is computationally efficient (one-shot calculation) and is guaranteed to be safe (though it may be more conservative).

## 3.3 Main Guarantees: Safety, Stability, and Convergence

We start our analysis by stating our episodic safety guarantees which are proven in Appendix C.3.

**Theorem 1** (Per-Episode Safety Guarantee). Let the system in equation (1) be given, Assumptions 1 and 2 hold, and  $r_{i+1}$  follow the implicit safety requirement (11). Then

$$\mathbb{P}_{n_i} \{ \mathbb{P} \{ s(\hat{y}_{0:T}, y_{j+1,0:T}) \le r_{j+1} \} \ge 1 - \alpha \} \ge 1 - \delta.$$
 (13)

Furthermore, if  $P[j+1; r_{j+1}]$  is feasible, then

$$\mathbb{P}_{n_i} \{ \mathbb{P} \{ H(x_{j+1,0:T}, y_{j+1,0:T}) \le 0 \} \ge 1 - \alpha \} \ge 1 - \delta.$$
 (14)

If H is Lipschitz continuous with Lipschitz constant  $L_H$ , we note that a sufficient condition for the feasibility of  $\mathbf{P}[j+1; r_{j+1}]$  is that  $H(x_{j+1,0:T}, \hat{y}_{0:T}) \leq -L_H r_{j+1}$ , see Appendix C.4.

We proceed our analysis using the explicit solver for the implicit inequality (11) which resulted in the tractable inequality in (12). We show its solution next and present the proof in Appendix C.5.

**Lemma 3** (Safe Explicit Radius Update). Let  $\kappa < 1$ . The minimal (i.e., least conservative) radius  $r_{j+1}$  that satisfies the tractable inequality (12) is given by the following closed-form solution:

$$r_{j+1} = \begin{cases} \frac{q_j + \kappa r_j}{1 + \kappa} & \text{if } q_j \le r_j \quad (Shrinkage Branch) \\ \frac{q_j - \kappa r_j}{1 - \kappa} & \text{if } q_j > r_j \quad (Expansion Branch) \end{cases}$$

$$(15)$$

If we limit  $r_{j+1}$  to an admissible interval  $\mathcal{R} = [r_{\min}, r_{\max}]$  (e.g., as needed in Appendix C.2 to derive  $L_U$ ), then we can project  $r_{j+1}$  onto  $\mathcal{R}$  via the operator  $\Pi_{\mathcal{R}}(r_{j+1}) = \min(r_{\max}, \max(r_{\min}, r_{j+1}))$ . This update rule leads to the following guarantees, for which we provide the proof in Appendix C.6.

**Theorem 2** (Episode-to-Episode Stability and Shrinkage). Let  $\kappa < 1$  and the radius  $r_{j+1}$  satisfy equation (15). Then, the per-episode change in the radius  $r_{j+1}$  is bounded by:

$$|r_{j+1} - r_j| \le \frac{1}{1 - \kappa} |q_j - r_j|.$$

Furthermore, if  $q_j < r_j$ , then it holds that  $r_{j+1} < r_j$ .

Finally, we analyze conditions under which our algorithms converge. We study the true quantile of the nonconformity score  $s(\hat{y}_{0:T}, y_{0:T})$  for  $y_{0:T} \sim \mathcal{D}(\pi^{\star}(r))$ . For simplicity, let

$$F_r(t) := \mathbb{P}\{s(\hat{y}_{0:T}, y_{i+1:0:T}) \le t\}$$

denote the cumulative distribution function (CDF) of the score and define the true quantile as

$$Q_{1-\alpha}(\pi^{\star}(r)) := \inf\{t \in \mathbb{R} : F_s(t) \ge 1 - \alpha\}.$$

We now analyze the error between true and empirical quantiles across episodes and provide the proof in Appendix C.7.

**Theorem 3** (Convergence with explicit error summation). Let  $T(r) := Q_{1-\alpha}(\pi^*(r))$  denote the  $(1-\alpha)$  true quantile of the nonconformity score. Assume that T(r) is Lipschitz continuous so that

$$|T(r) - T(r')| \le \kappa |r - r'|$$
 for all  $r, r' \in \mathbb{R}_{\ge 0}$ ,  $\kappa = \beta_T L_U \in (0, 1)$ .

Suppose further that there is a fixed point  $r^* \in \mathbb{R}_{\geq 0}$  with  $T(r^*) = r^*$ . At episode j, let the radius  $r_{j+1}$  satisfy equation (15). Define  $e_j = |r_j - r^*|$  and  $\eta_j = q_j - T(r_j)$ . Then, the following hold:

(U) Finite-horizon error bound. At each episode j, we are guaranteed that

$$e_{j+1} \le \gamma_{\kappa}^{j+1} e_0 + B_{\kappa} \sum_{m=0}^{j} \gamma_{\kappa}^{j-m} |\eta_m| \qquad \gamma_{\kappa} = \frac{2\kappa}{1-\kappa}, \quad B_{\kappa} = \frac{1}{1-\kappa}, \qquad \gamma_{\kappa} < 1 \iff \kappa < \frac{1}{3}. \quad (16)$$

(C) Closed form under a uniform perturbation bound. If  $|\eta_m| \le C$  for all  $m \in \{0, ..., j\}$ , then

$$e_{j+1} \le \gamma_{\kappa}^{j+1} e_0 + B_{\kappa} C \frac{1 - \gamma_{\kappa}^{j+1}}{1 - \gamma_{\kappa}}, \quad \text{and, if } \kappa < \frac{1}{3} : \limsup_{j \to \infty} e_j \le \frac{B_{\kappa}}{1 - \gamma_{\kappa}} C = \frac{1}{1 - 3\kappa} C.$$
 (17)

(HP- $\eta$ ) High-probability control of  $\eta_j$ . If the CDF  $F_{r_j}(s)$  is differentiable and has density  $f_{r_j}(s)$  no less than  $f_{\star} > 0$  for all s in a sufficiently large neighborhood of its  $(1 - \alpha)$  quantile  $Q_{1-\alpha}(\pi^{\star}(r_j))$ , then for any failure probability  $\delta_j \in (0,1)$  we have

$$\mathbb{P}_{n_j} \left\{ |\eta_j| \le \frac{|\alpha - \bar{\alpha}_j|}{f_{\star}} + \frac{1}{f_{\star}} \sqrt{\frac{\ln(2/\delta_j)}{2n_j}} \right\} \ge 1 - \delta_j. \tag{18}$$

Furthermore, we get

$$\mathbb{P}_{\sum_{m=0}^{j} n_{m}} \left\{ e_{j+1} \leq \gamma_{\kappa}^{j+1} e_{0} + \frac{B_{\kappa}}{f_{\star}} \sum_{m=0}^{j} \gamma_{\kappa}^{j-m} |\alpha - \bar{\alpha}_{m}| + \frac{B_{\kappa}}{f_{\star}} \sum_{m=0}^{j} \gamma_{\kappa}^{j-m} \sqrt{\frac{\ln(2/\delta_{m})}{2n_{m}}} \right\} \geq 1 - \sum_{m=0}^{j} \delta_{m}. \tag{19}$$

(A) Asymptotics. If  $n_j \to \infty$  and  $\bar{\alpha}_j \to \alpha$ , then  $|\eta_j| \to 0$  and for  $\kappa < \frac{1}{3}$  we have  $e_j \to 0$  (hence  $r_j \to r^*$ ). If instead  $\bar{\alpha}_j \equiv \bar{\alpha} < \alpha$  and  $n_j \to \infty$ , then  $|\eta_j| \to (\alpha - \bar{\alpha})/f_*$  and (17) yields a conservative limit of size at most  $\frac{1}{1-3\kappa} \cdot \frac{\alpha-\bar{\alpha}}{f_*}$  around  $r^*$ .

# 4 Case study

We now instantiate the 2D car-pedestrian example from the paper. The ego car  $x_t \in \mathbb{R}^2$  follows single-integrator dynamics  $x_{t+1} = x_t + \Delta u_t$  with sampling time  $\Delta := 0.1$  and component-wise control bounds  $\|u_t\|_{\infty} \leq u_{\max} := 2$ . The pedestrian  $y_t \in \mathbb{R}^2$  follows the interactive dynamics

$$y_{t+1} = y_t + \Delta(v_0 + \phi(||r_t||_2)e_t) + w_t$$

where  $r_t := y_t - x_t$  is the relative position between the car and the pedestrian,  $e_t := r_t/\|r_t\|_2$  is the normalized relative position,  $v_0 := \begin{bmatrix} -0.5 & 0 \end{bmatrix}^T$  is the normalized velocity, and  $w_t \sim \mathcal{N}(0, \Delta \sigma^2 I)$  is random Gaussian noise with variance  $\sigma := 0.05$ . The interaction function  $\phi(\|r_k\|_2) := v_{\max} \frac{\ell_c^2}{\|r_k\|_2^2 + \ell_c^2}$  models a repulsive force with maximal "fleeing" speed  $v_{\max} := 1$  and interaction distance  $\ell_c := 1$ . Our predictor

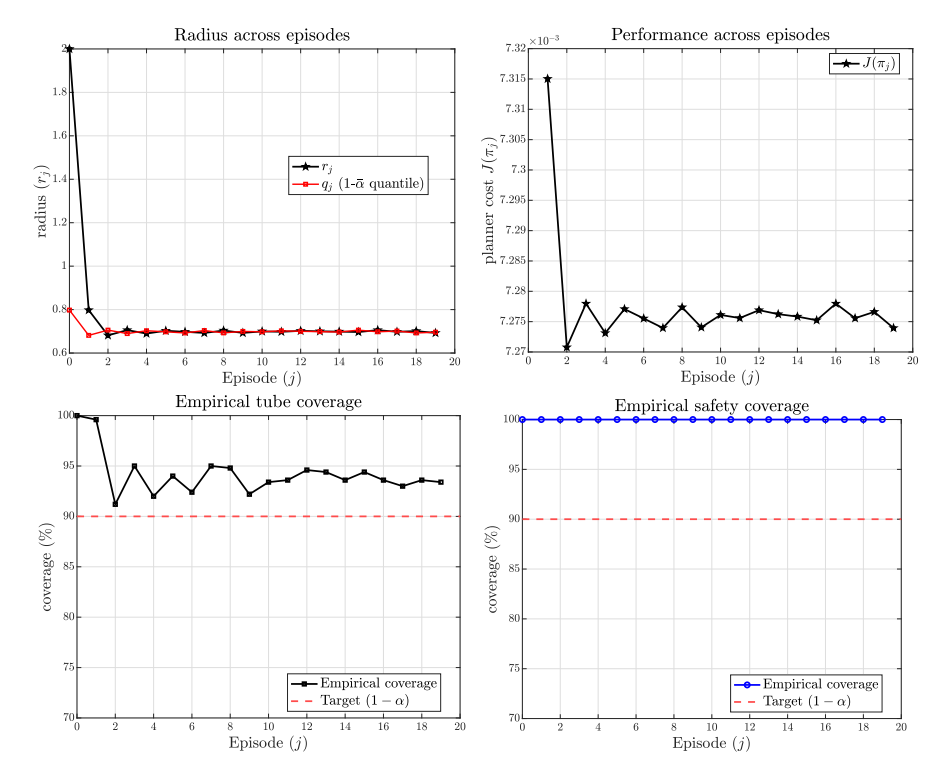


Figure 3: 2D car-pedestrian example. Top left: convergence of tube radius  $r_j$  over episodes j, top right: convergence of performance  $J_j$ , bottom left: empirical coverage of  $\mathbb{P}\left\{y_{j,0:T} \in \mathcal{C}_{r_j}\right\}$ , and bottom right: empirical coverage of safety  $\mathbb{P}\left\{H(x_{j,0:T},y_{j,0:T}) \leq 0\right\}$ .

has no access to this interaction function and is constructed as  $\hat{y}_{t+1} = \hat{y}_t + \Delta v_0$  with initial condition  $\hat{y}_0 := y_0 := \begin{bmatrix} 3 & 1.5 \end{bmatrix}^T$ .

The planner in this case study minimizes the cost function

$$J(x, u) := w_{\text{goal}} \|x_T - x_{\text{goal}}\|_2^2 + w_{\text{track}} \sum_{t=0}^{T-1} \|u_t\|^2$$

with goal position  $x_{\rm goal} := \begin{bmatrix} 6 & 0.5 \end{bmatrix}^T$ , weights  $w_{\rm goal} := 1$  and  $w_{\rm track} := 0.0001$ , and time horizon T := 5. The safety function is  $H(x,y) := \max_{0 \le t \le T} d_{\min} - \|x_t - y_t\|_2$  where  $d_{\min} := 0.8$  is the minimum safety distance. For our iterative algorithm we choose the failure probabilities  $\alpha := 0.1$  and  $\delta := 0.05$ . For recalibration, we use  $n_j := 1000$  trajectories.

Our analysis relies on the assumption that  $\kappa < 1$ . Because this condition is sometimes violated in our experimental settings, we estimate  $\kappa$  and use it as a tunable parameter to improve performance. Although this deviates from our results, the resulting update rule for  $r_j$  remains well-motivated and principled as it directly follows from our theory developed under  $\kappa < 1$ . Indeed, we use  $\kappa_j = \beta_T(\pi_j) \, L_U(\pi_j)$  where  $L_U(\pi_j) \approx \|\pi^\star(r_j + \delta) - \pi^\star(r_j - \delta)\|_{\infty}/2\delta$  is a local Lipschitz estimate of  $\pi^\star(r)$ . In parallel, we estimate the sensitivity  $\beta_T(\pi_j) \approx \max_{0 \le t \le T} \|y_t(\pi_j + \Delta \pi) - y_t(\pi_j - \Delta \pi)\|_2/2 \|\Delta \pi\|_{\infty}$ , via symmetric finite differences of rollouts under  $\pi_j \pm \Delta \pi$ ,

In Figure 3, we report the radius  $r_j$ , the cost  $J_J$ , the empirical tube coverage  $\mathbb{P}\left\{y_{j,0:T} \in \mathcal{C}_{r_j}\right\}$ , and the

empirical safety coverage  $\mathbb{P}\left\{H(x_{j,0:T},y_{j,0:T})\leq 0\right\}$  over episodes j. We observe that the tube radius and the performance converge after a few episodes. Importantly, we also observe that empirical coverage for the tube and the safety function are maintained across episodes.

# References

- [1] C. Mavrogiannis, F. Baldini, A. Wang, D. Zhao, P. Trautman, A. Steinfeld, and J. Oh, "Core challenges of social robot navigation: A survey," *ACM Transactions on Human-Robot Interaction*, vol. 12, no. 3, pp. 1–39, 2023.
- [2] Z. Feng, R. Xue, L. Yuan, Y. Yu, N. Ding, M. Liu, B. Gao, J. Sun, and G. Wang, "Multi-agent embodied ai: Advances and future directions," 2025. [Online]. Available: https://arxiv.org/abs/2505.05108
- [3] P. Trautman and A. Krause, "Unfreezing the robot: Navigation in dense, interacting crowds," in 2010 IEEE/RSJ International Conference on Intelligent Robots and Systems. IEEE, 2010, pp. 797–803.
- [4] N. E. Du Toit and J. W. Burdick, "Robot motion planning in dynamic, uncertain environments," *IEEE Transactions on Robotics*, vol. 28, no. 1, pp. 101–115, 2011.
- [5] H. Kretzschmar, M. Spies, C. Sprunk, and W. Burgard, "Socially compliant mobile robot navigation via inverse reinforcement learning," *The Int. Journal Robot. Research*, vol. 35, no. 11, pp. 1289–1307, 2016.
- [6] M. Everett, Y. F. Chen, and J. P. How, "Collision avoidance in pedestrian-rich environments with deep reinforcement learning," *IEEE Access*, vol. 9, pp. 10357–10377, 2021.
- [7] V. Vovk, A. Gammerman, and G. Shafer, *Algorithmic learning in a random world*. Springer, 2005, vol. 29.
- [8] A. N. Angelopoulos and S. Bates, "A gentle introduction to conformal prediction and distribution-free uncertainty quantification," *arXiv* preprint arXiv:2107.07511, 2021.
- [9] M. Cleaveland, I. Lee, G. J. Pappas, and L. Lindemann, "Conformal prediction regions for time series using linear complementarity programming," in *Proceedings of the AAAI Conference on Artificial Intelligence*, vol. 38, no. 19, 2024, pp. 20984–20992.
- [10] S. Sun and R. Yu, "Copula conformal prediction for multi-step time series forecasting," *arXiv preprint* arXiv:2212.03281, 2022.
- [11] M. Zecchin, S. Park, and O. Simeone, "Forking uncertainties: Reliable prediction and model predictive control with sequence models via conformal risk control," *IEEE Journal on Selected Areas in Information Theory*, vol. 5, pp. 44–61, 2024.
- [12] L. Lindemann, M. Cleaveland, G. Shim, and G. J. Pappas, "Safe planning in dynamic environments using conformal prediction," *IEEE Robotics and Automation Letters*, vol. 8, no. 8, pp. 5116–5123, 2023.
- [13] A. Dixit, L. Lindemann, S. X. Wei, M. Cleaveland, G. J. Pappas, and J. W. Burdick, "Adaptive conformal prediction for motion planning among dynamic agents," in *Proceedings*

- of The 5th Annual Learning for Dynamics and Control Conference, ser. Proceedings of Machine Learning Research, vol. 211. PMLR, 2023, pp. 300–314. [Online]. Available: https://proceedings.mlr.press/v211/dixit23a.html
- [14] J. Shin, J. Lee, and I. Yang, "Egocentric conformal prediction for safe and efficient navigation in dynamic cluttered environments," *arXiv preprint arXiv:2504.00447*, 2025.
- [15] J. Yao, X. Zhang, Y. Xia, Z. Wang, A. K. Roy-Chowdhury, and J. Li, "Sonic: Safe social navigation with adaptive conformal inference and constrained reinforcement learning," *arXiv* preprint *arXiv*:2407.17460, 2024.
- [16] J. Sun, Y. Jiang, J. Qiu, P. Nobel, M. J. Kochenderfer, and M. Schwager, "Conformal prediction for uncertainty-aware planning with diffusion dynamics model," *Advances in Neural Information Process*ing Systems, vol. 36, pp. 80 324–80 337, 2023.
- [17] J. Zhang, B. Hoxha, G. Fainekos, and D. Panagou, "Conformal prediction in the loop: Risk-aware control barrier functions for stochastic systems with data-driven state estimators," *IEEE Control Systems Letters*, 2025.
- [18] T.-W. Hsu and H. Tsukamoto, "Statistical guarantees in data-driven nonlinear control: Conformal robustness for stability and safety," *IEEE Control Systems Letters*, 2025.
- [19] S. Sheng, P. Yu, D. Parker, M. Kwiatkowska, and L. Feng, "Safe pomdp online planning among dynamic agents via adaptive conformal prediction," *IEEE Robotics and Automation Letters*, 2024.
- [20] A. Doula, M. Mühlhäuser, and A. S. Guinea, "Safepath: Conformal prediction for safe llm-based autonomous navigation," *arXiv* preprint arXiv:2505.09427, 2025.
- [21] J. Wang, G. He, and Y. Kantaros, "Probabilistically correct language-based multi-robot planning using conformal prediction," *IEEE Robotics and Automation Letters*, 2024.
- [22] L. Lindemann, Y. Zhao, X. Yu, G. J. Pappas, and J. V. Deshmukh, "Formal verification and control with conformal prediction," *arXiv preprint arXiv:2409.00536*, 2024.
- [23] R. J. Tibshirani, R. Foygel Barber, E. Candes, and A. Ramdas, "Conformal prediction under covariate shift," *Advances in neural information processing systems*, vol. 32, 2019.
- [24] Y. Zhao, B. Hoxha, G. Fainekos, J. V. Deshmukh, and L. Lindemann, "Robust conformal prediction for stl runtime verification under distribution shift," in 2024 ACM/IEEE 15th International Conference on Cyber-Physical Systems (ICCPS). IEEE, 2024, pp. 169–179.
- [25] I. Gibbs and E. Candes, "Adaptive conformal inference under distribution shift," in *Advances in Neural Information Processing Systems*, vol. 34, 2021, pp. 1660–1672.
- [26] M. Zaffran, O. Féron, Y. Goude, J. Josse, and A. Dieuleveut, "Adaptive conformal predictions for time series," in *International Conference on Machine Learning*. PMLR, 2022, pp. 25 834–25 866.
- [27] Y. Yang, A. K. Kuchibhotla, and E. Tchetgen Tchetgen, "Doubly robust calibration of prediction sets under covariate shift," *Journal of the Royal Statistical Society Series B: Statistical Methodology*, vol. 86, no. 4, pp. 943–965, 2024.

- [28] S. Alijani and H. Najjaran, "Wqlcp: Weighted adaptive conformal prediction for robust uncertainty quantification under distribution shifts," 2025. [Online]. Available: https://arxiv.org/abs/2505.19587
- [29] M. Cauchois, S. Gupta, A. Ali, and J. C. Duchi, "Robust validation: Confident predictions even when distributions shift," *Journal of the American Statistical Association*, vol. 119, no. 548, pp. 3033–3044, 2024.
- [30] L. Aolaritei, Z. O. Wang, J. Zhu, M. I. Jordan, and Y. Marzouk, "Conformal prediction under levy-prokhorov distribution shifts: Robustness to local and global perturbations," *arXiv preprint arXiv:2502.14105*, 2025.
- [31] A. Gendler, T. Weng, L. Daniel, and Y. Romano, "Adversarially robust conformal prediction," in *Proceedings of the International Conference on Learning Representations (ICLR)*, 2022, openReview ID: 9L1BsI4wP1H. [Online]. Available: https://openreview.net/forum?id=9L1BsI4wP1H
- [32] S. Tonkens, S. Sun, R. Yu, and S. Herbert, "Scalable safe long-horizon planning in dynamic environments leveraging conformal prediction and temporal correlations," in *Long-Term Human Motion Prediction Workshop, International Conference on Robotics and Automation*, 2023.
- [33] X. Yu, Y. Zhao, X. Yin, and L. Lindemann, "Signal temporal logic control synthesis among uncontrollable dynamic agents with conformal prediction," *Automatica*, vol. 183, p. 112616, 2026. [Online]. Available: https://www.sciencedirect.com/science/article/pii/S0005109825005126
- [34] Z. Huang, T. Ji, H. Zhang, F. C. Pouria, K. Driggs-Campbell, and R. Dong, "Interaction-aware conformal prediction for crowd navigation," *arXiv preprint arXiv:2502.06221*, 2025.
- [35] S. Wang, Y. Gao, and X. Yin, "Learning-based conformal tube mpc for safe control in interactive multi-agent systems," *arXiv preprint arXiv:2504.03293*, 2025.
- [36] V. Vovk, "Conditional validity of inductive conformal predictors," in *Asian conference on machine learning*. PMLR, 2012, pp. 475–490.

# A The Iterative Policy Update Algorithm

### Algorithm 1 Iterative Safe Policy Improvement (Explicit & Implicit Forms)

```
1: Input: confidence levels 1 - \alpha, 1 - \delta; initial safe policy \pi_0.
 2: Input: closed-loop gain \kappa = \beta_T L_U; fixed predictor \hat{y}_T.
 3: Input: Solver choice: SOLVER_TYPE ∈ {'EXPLICIT', 'IMPLICIT'}.
 4: Initialize: Choose r_0 \in \mathcal{R}; set \pi_0 \leftarrow \pi^*(r_0).
 5: for j = 0, 1, 2, \dots do
        Execute \pi_j; collect rollouts \{y_{j,0:T}^{(i)}\}_{i=1}^{n_j}.
        Calibration level with \delta inside: \bar{\alpha}_j \leftarrow \alpha - \sqrt{\frac{\ln(1/\delta)}{2n_j}}, so that \bar{\alpha}_j \in (0, \alpha).
 7:
        Empirical quantile (scores at episode j): q_j \leftarrow q_{1-\bar{\alpha}_j} \Big( \big\{ s(\hat{y}_{0:T}, y_{j,0:T}^{(i)}) \big\}_{i=1}^{n_j} \Big).
 8:
        if SOLVER TYPE = 'EXPLICIT' then
 9:
           {Use analytical solution from Thm. 3}
10:
11:
           if q_j \leq r_j then
              r_{j+1} \leftarrow (q_j + \kappa r_j)/(1 + \kappa)
12:
13:
              r_{j+1} \leftarrow (q_j - \kappa r_j)/(1 - \kappa)
14:
           end if
15:
        else if SOLVER_TYPE = 'IMPLICIT' then
16:
           {Use iterative solver for Eq. (11)}
17:
           r_{j+1} \leftarrow \text{FindRoot}(r \mapsto r - (q_j + \beta_T \|\pi^*(r) - \pi_j\|_{\infty}))
18:
19:
        Certify and Deploy: Solve P[j+1; r_{j+1}] to get policy \pi_{j+1} \leftarrow \pi^*(r_{j+1}).
20:
21:
        Monitor: Record |r_{j+1}-r_j| and ||\pi_{j+1}-\pi_j||_{\infty}.
        if changes are below threshold then break.
22:
23: end for
```

# **B** The Implicit Solver Algorithm

- 1. Start with a search range  $[r_{low}, r_{high}] = [q_j, r_{max}]$ .
- 2. Propose a candidate radius  $r_{\text{cand}} = (r_{\text{low}} + r_{\text{high}})/2$ .
- 3. Call the planner (the "pi\_cand" step): Solve  $P[j+1; r_{cand}]$  to get the candidate policy  $\pi_{cand} = \pi^*(r_{cand})$ .
- 4. Check the inequality: Calculate the true required budget for this policy:  $M_{\text{req}} = \beta_T \|\pi_{\text{cand}} \pi_j\|_{\infty}$ .
- 5. If  $r_{\rm cand} \ge q_j + M_{\rm req}$ , the radius is safe. This is a valid solution, so we try to find a smaller one:  $r_{\rm high} = r_{\rm cand}$ .

- 6. If  $r_{\text{cand}} < q_j + M_{\text{req}}$ , the radius is unsafe. We must search higher:  $r_{\text{low}} = r_{\text{cand}}$ .
- 7. Repeat until the range is sufficiently small. The final  $r_{j+1}$  is  $r_{high}$ .

# C Deferred Proofs

#### C.1 Proof of Lemma 2

Let us first recall the dynamics of ego and uncontrollable agents from (1) as

$$x_{t+1} = f_X(x_t, u_t), y_{t+1} = f_Y(y_t, x_t, u_t, \nu_t),$$

under the noise sequence  $\{\nu_t\}_{t=0}^{T-1}$ . Under Assumption 1, i.e., Lipschitz continuity of  $f_X$  and  $f_Y$ , our goal is now to bound the deviation in the environment trajectory from  $y_{0:T}$  to  $y'_{0:T}$  caused by a change in the policy from  $\pi = \{u_t\}_{t=1}^{T-1}$  to  $\pi' = \{u'_t\}_{t=1}^{T-1}$ . Indeed, we want to show that

$$||x_{0:T} - x'_{0:T}||_{\infty} \le A_T \Delta u, \qquad A_T := L_{Xu} \sum_{t=0}^{T-1} (L_{Xx})^t,$$
 (20)

$$||y_{0:T} - y'_{0:T}||_{\infty} \le \beta_T \Delta u, \qquad \beta_T := (L_{Yx} A_T + L_{Yu}) \sum_{t=0}^{T-1} (L_{Yy})^t.$$
(21)

where  $\Delta u := \|\pi - \pi'\|_{\infty}$  with  $\|\pi - \pi'\|_{\infty} := \max_{0 \le t \le N-1} \|u_t - u_t'\|_{2}$ .

*Proof.* Let  $\Delta x_t := x_t - x_t'$ ,  $\Delta y_t := y_t - y_t'$ , and  $\Delta u_t := u_t - u_t'$ . From Assumption 1, we get

$$\|\Delta x_{t+1}\|_{2} \le L_{Xx} \|\Delta x_{t}\|_{2} + L_{Xu} \|\Delta u_{t}\|_{2}. \tag{22}$$

Unrolling (22) until time t with  $\Delta x_0 = 0$  and  $\|\Delta u_t\|_2 \leq \Delta u$  then gives

$$\|\Delta x_t\|_2 \le L_{Xu} \sum_{i=0}^{t-1} (L_{Xx})^i \Delta u.$$
 (23)

Since all Lipschitz constants are nonnegative, the partial sum in (23) is monotone in t so that

$$||x_{0:T} - x'_{0:T}||_{\infty} = \max_{0 \le t \le T} ||\Delta x_t||_2 = ||\Delta x_T||_2 \le L_{Xu} \sum_{t=0}^{T-1} (L_{Xx})^t \Delta u,$$

which proves (20). Next, from Assumption 1, we get

$$\|\Delta y_{t+1}\|_2 \le L_{Yu} \|\Delta y_t\|_2 + L_{Yu} \|\Delta x_t\|_2 + L_{Yu} \|\Delta u_t\|_2.$$

Using (23) and  $\|\Delta u_t\|_2 \leq \Delta u$ , it the follows that

$$\|\Delta y_{t+1}\|_{2} \le L_{Yu} \|\Delta y_{t}\|_{2} + (L_{Yx}A_{T} + L_{Yu})\Delta u. \tag{24}$$

Unrolling (24) until time t with  $\Delta y_0 = 0$  then gives

$$\|\Delta y_t\|_2 \le (L_{Yx}A_T + L_{Yu}) \sum_{i=0}^{t-1} (L_{Yy})^i \Delta u.$$

Again by nonnegativity of the Lipschitz constants, this sum is monotone in t so that

$$||y_{0:T} - y'_{0:T}||_{\infty} = ||\Delta y_T||_2 \le (L_{Yx}A_T + L_{Yu}) \sum_{t=0}^{T-1} (L_{Yy})^t \Delta u,$$

which proves (21), what was to be shown.

### C.2 Derivation of Planner Sensitivity $L_U$

**Proposition 1** (Planner Regularity & Lipschitzness). Assume there exists a compact interval of radii  $\mathcal{R} := [r_{\min}, r_{\max}]$  such that for all  $r \in \mathcal{R}$ , the robust planning problem  $\mathbf{P}[j; r_j]$  in (5) is feasible, convex, and has a unique, regular optimizer  $\pi^*(r)$  satisfying standard KKT conditions (LICQ, strict complementarity, and a nonsingular KKT matrix). Then the solution map  $r \mapsto \pi^*(r)$  is locally Lipschitz on  $\mathcal{R}$ . In particular, there exists a uniform constant  $L_U < \infty$  such that

$$\|\pi^*(r) - \pi^*(r')\|_{\infty} \le L_U |r - r'|, \quad \forall r, r' \in \mathcal{R}.$$
 (25)

*Proof.* We derive  $L_U$  via parametric sensitivity of  $\mathbf{P}[j;r]$  in (5). Throughout, we assume the inequality constraints depend affinely on the radius,

$$a_k(\pi) + b_k r \le 0 \quad (k = 1, \dots, m),$$

and any equality constraints  $h(\pi) = 0$  do not depend on r.

Active set and multipliers. Fix  $r \in \mathcal{R}$  and let  $\pi^*(r)$  denote the unique optimizer. Define the active set

$$\mathcal{A}(r) := \{ k : a_k(\pi^*(r)) + b_k r = 0 \},$$

and let  $\lambda_k^*(r) > 0$  be the corresponding Lagrange multipliers for  $k \in \mathcal{A}(r)$  (strict complementarity). Let  $\mu^*(r)$  be the multipliers for  $h(\pi) = 0$  (if present).

<sup>&</sup>lt;sup>5</sup>For instance, this is the case for the program in (5) when H is Lipschitz continuous with Lipschitz constant  $L_H$  so that  $H(x_{j,0:T},\zeta) \leq 0 \quad \forall \zeta \in \mathcal{C}_{r_j}(\hat{y}_{0:T})$  can be rewritten as  $H(x_{j,0:T},\hat{y}_{0:T}) \leq -L_H r_j$  (see Appendix C.4).

<sup>&</sup>lt;sup>6</sup>If h (or the gradients of  $a_k$ ) depend on r, the derivative formula below includes additional right-hand-side terms; see Remark 1. The Lipschitz conclusion (25) is unchanged under strong regularity.

**Second-order objects.** Define the Hessian of the Lagrangian, the Jacobian of active constraints, and the vector of active radius coefficients:

$$H(r) := \nabla_{\pi\pi}^2 J(\pi^*(r)) + \sum_{k \in \mathcal{A}(r)} \lambda_k^*(r) \, \nabla_{\pi\pi}^2 a_k(\pi^*(r)), \tag{26}$$

$$G_{\mathcal{A}}(r) := \left[ \nabla_{\pi} a_k(\pi^*(r)) \right]_{k \in \mathcal{A}(r)} \in \mathbb{R}^{|\mathcal{A}(r)| \times n}, \tag{27}$$

$$b_{\mathcal{A}}(r) := \left[ b_k \right]_{k \in \mathcal{A}(r)} \in \mathbb{R}^{|\mathcal{A}(r)|}. \tag{28}$$

If equalities are present, let  $E(r) := \nabla_{\pi} h(\pi^*(r))$ .

**KKT conditions.** At  $(\pi^*, \lambda^*, \mu^*; r)$  the KKT conditions read

$$\nabla_{\pi} J(\pi^*(r)) + \sum_{k \in \mathcal{A}(r)} \lambda_k^*(r) \, \nabla_{\pi} a_k(\pi^*(r)) + E(r)^{\top} \mu^*(r) = 0, \tag{29}$$

$$a_k(\pi^*(r)) + b_k r \le 0 \ (k = 1, ..., m), \qquad h(\pi^*(r)) = 0,$$
 (30)

$$\lambda_k^*(r) \ge 0 \ (k = 1, \dots, m), \qquad \lambda_k^*(r) \left( a_k(\pi^*(r)) + b_k r \right) = 0 \ (k = 1, \dots, m).$$
 (31)

Under LICQ, strict complementarity, and the second-order condition, the KKT matrix is nonsingular (strong regularity), and the active set A(r) is locally constant.

**Linearized KKT system.** Differentiate (29)–(31) with respect to r over any subinterval where  $\mathcal{A}(r)$  is fixed. With  $E \equiv E(r)$  and dropping the explicit r for brevity,

$$\begin{bmatrix} H & G_{\mathcal{A}}^{\top} & E^{\top} \\ G_{\mathcal{A}} & 0 & 0 \\ E & 0 & 0 \end{bmatrix} \begin{bmatrix} \frac{d\pi^*}{dr} \\ \frac{d\lambda_{\mathcal{A}}^*}{dr} \\ \frac{d\mu^*}{dr} \end{bmatrix} = \begin{bmatrix} 0 \\ -b_{\mathcal{A}} \\ 0 \end{bmatrix}.$$
 (32)

Nonsingularity of the KKT matrix (strong regularity) ensures a unique solution to (32).

**Sensitivity formula.** Eliminate multipliers in (32) via the Schur complement. If no equalities are present (E=0), we obtain the classical expression

$$\frac{d\pi^*(r)}{dr} = -H(r)^{-1} G_{\mathcal{A}}(r)^{\top} \left( G_{\mathcal{A}}(r) H(r)^{-1} G_{\mathcal{A}}(r)^{\top} \right)^{-1} b_{\mathcal{A}}(r). \tag{33}$$

With equalities, replace  $G_{\mathcal{A}}$  by  $W(r) := \begin{bmatrix} G_{\mathcal{A}}(r) \\ E(r) \end{bmatrix}$  and  $b_{\mathcal{A}}$  by  $c_{\mathcal{A}}(r) := \begin{bmatrix} b_{\mathcal{A}}(r) \\ 0 \end{bmatrix}$  in (33).

**Uniform bound and Lipschitz continuity.** Define

$$L_U := \sup_{r \in \mathcal{R}} \left\| H(r)^{-1} G_{\mathcal{A}}(r)^{\top} \left( G_{\mathcal{A}}(r) H(r)^{-1} G_{\mathcal{A}}(r)^{\top} \right)^{-1} b_{\mathcal{A}}(r) \right\|_{\infty}. \tag{34}$$

Continuity of the matrices in (26)–(28) and uniform nonsingularity on each fixed-active-set region imply the supremum in (34) is finite. The mean-value theorem then yields (25).

**Remark 1** (Radius-dependent data). If  $h(\pi,r)$  depends on r or if  $\nabla_{\pi}a_k(\pi,r)$  depends on r, the right-hand side of (32) becomes  $\begin{bmatrix} g^{\top}, -b_{\mathcal{A}}^{\top}, -d_h^{\top} \end{bmatrix}^{\top}$ , where  $g := \partial_r (\nabla_{\pi}J + \sum_{k \in \mathcal{A}} \lambda_k^* \nabla_{\pi}a_k + E^{\top}\mu^*)$  and  $d_h := \partial_r h(\pi^*, r)$ . The proof proceeds identically, and the Lipschitz property (25) continues to hold under strong regularity.

#### C.3 Proof of Theorem 1

Let  $y_{j+1,0:T}$  and  $y_{j,0:T}$  be trajectories generated by the control policies  $\pi_{j+1}$  and  $\pi_j$  in episodes j+1 and j, respectively. Recall from our previous discussion and Lemma 2 that

$$||y_{j+1,0:T} - y_{j,0:T}||_{\infty} \le \beta_T ||\pi_{j+1} - \pi_j||_{\infty}.$$
 (35)

The nonconformity score s defined in (3) has Lipschitz constant one so that we have

$$|s(\hat{y}_{0:T}, y_{i,0:T}) - s(\hat{y}_{0:T}, y_{i+1,0:T})| \le \beta_T \|\pi_{i+1} - \pi_i\|_{\infty}.$$

Next, applying adversarial CP from Lemma 1 immediately results in the guarantee

$$\mathbb{P}_{n,i} \{ \mathbb{P} \{ s(\hat{y}_{0:T}, y_{i+1,0:T}) \leq q_i + \beta_T \| \pi_{i+1} - \pi_i \|_{\infty} \} \geq 1 - \alpha \} \geq 1 - \delta.$$

Since the implicit safety requirement in (11) holds by assumption, we know that  $r_{j+1} \ge q_j + \beta_T \|\pi^*(r_{j+1}) - \pi_j\|_{\infty}$  is satisfied. This in turn implies that

$$\mathbb{P}_{n_j} \{ \mathbb{P} \{ s(\hat{y}_{0:T}, y_{j+1,0:T}) \le r_{j+1} \} \ge 1 - \alpha \} \ge 1 - \delta, \tag{36}$$

which was the first result in equation (13) that was to be shown.

Assume now that the optimization problem  $P[j+1; r_{j+1}]$  in (5) is feasible. This means that

$$H(x_{j+1,0:T},\zeta) \le 0 \quad \forall \zeta \in \mathcal{C}_{r_{j+1}}(\hat{y}_{0:T})$$

$$\tag{37}$$

where we recall that the set  $C_{r_{j+1}}(\hat{y}_{0:T})$  is defined as  $C_{r_{j+1}}(\hat{y}_{0:T}) := \{y_{0:T} : s(\hat{y}_{0:T}, y_{0:T}) \leq r_{j+1}\}$ . Combining (36) and (37) implies that

$$\mathbb{P}_{n_j} \{ \mathbb{P} \{ H(x_{j+1,0:T}, y_{j+1,0:T}) \le 0 \} \ge 1 - \alpha \} \ge 1 - \delta,$$

which was the second result in equation (14) that was to be shown.

# C.4 Sufficient Condition for Feasibility of $P[j+1; r_{j+1}]$ in (5)

First note that feasibility of the optimization problem  $P[j; r_j]$  in (5) is guaranteed if the constraint

$$H(x_{j,0:T},\zeta) \le 0 \quad \forall \zeta \in \mathcal{C}_{r_j}(\hat{y}_{0:T})$$
 (38)

is satisfied by the trajectory  $x_{j,0:T}$ , where we recall that  $\mathcal{C}_{r_j}(\hat{y}_{0:T}) = \{y_{0:T}: \|y_{0:T} - \hat{y}_{0:T}\|_{\infty} \leq r_j \}$ . Assume now that there exists a Lipschitz constant  $L_H \geq 0$  such that

$$|H(x_{0:T}, y_{0:T}) - H(x_{0:T}, y'_{0:T})| \le L_H ||y_{0:T} - y'_{0:T}||_{\infty}$$

for all permissible  $x_{0:T}$  and all  $y_{0:T}$ ,  $y'_{0:T}$ . Consequently, if the trajectory  $x_{j,0:T}$  satisfies

$$H(x_{j,0:T}, \hat{y}_{0:T}) \leq -L_H r_j,$$

then, for any  $y_{0:T} \in \mathcal{C}_{r_i}(\hat{y}_{0:T})$ , we know that

$$H(x_{j,0:T}, y_{0:T}) \le H(x_{j,0:T}, \hat{y}_{0:T}) + \left| H(x_{j,0:T}, y_{0:T}) - H(x_{j,0:T}, \hat{y}_{0:T}) \right|$$

$$\le -L_H r_j + L_H \|y_{0:T} - \hat{y}_{0:T}\|_{\infty} \le -L_H r_j + L_H r_j = 0,$$

by which we have shown that (38) is satisfied so that  $P[j; r_j]$  is feasible.

#### C.5 Proof of Lemma 3

Our goal is to derive the solution to the tractable inequality in (12), which we recall for convenience:

$$r_{j+1} \ge q_j + \kappa |r_{j+1} - r_j|.$$
 (39)

By assumption, we have that  $\kappa < 1$ . Since the right-hand side of (39) is nondecreasing in  $r_{j+1}$ , the minimal solution is obtained by saturating (39). Due to the absolute value in  $|r_{j+1} - r_j|$  in (39), we have to consider the two cases of shrinkage  $(r_{j+1} \le r_j)$  and expansion  $(r_{j+1} > r_j)$ .

Case 1: Shrinkage  $(r_{j+1} \le r_j)$ . We have that  $|r_{j+1} - r_j| = r_j - r_{j+1}$  so that (39) becomes

$$r_{j+1} \geq q_j + \kappa (r_j - r_{j+1}) \iff (1+\kappa) r_{j+1} \geq q_j + \kappa r_j$$

Since  $1 + \kappa > 0$ , the minimal value of  $r_{j+1}$  saturates the inequality, i.e.,

$$r_{j+1} = \frac{q_j + \kappa r_j}{1 + \kappa}. (40)$$

Consistency with the shrinkage assumption requires

$$\frac{q_j + \kappa r_j}{1 + \kappa} \le r_j \iff q_j \le r_j.$$

Case 2: Expansion  $(r_{j+1} > r_j)$ . We have that  $|r_{j+1} - r_j| = r_{j+1} - r_j$  so that (39) becomes

$$r_{j+1} \geq q_j + \kappa (r_{j+1} - r_j) \iff (1 - \kappa) r_{j+1} \geq q_j - \kappa r_j.$$

Since  $1 - \kappa > 0$ , the minimal value of  $r_{j+1}$  saturates the inequality, i.e.,

$$r_{j+1} = \frac{q_j - \kappa r_j}{1 - \kappa}. (41)$$

Consistency with the expansion assumption requires

$$\frac{q_j - \kappa r_j}{1 - \kappa} > r_j \iff q_j > r_j.$$

In conclusion, the above condition partition the line by  $q_j \le r_j$  and  $q_j > r_j$ . Combining this with (40) and (41) yields the closed-form solution in (15), which was to be shown.

#### C.6 Proof of Theorem 2

We analyze the magnitude  $|r_{j+1} - r_j|$  in the same two cases considered in Theorem 3.

• Case 1: Shrinkage  $(q_j \le r_j)$ . We can derive that

$$|r_{j+1} - r_j| = r_j - r_{j+1} = r_j - \left(\frac{q_j + \kappa r_j}{1 + \kappa}\right) = \frac{r_j(1 + \kappa) - q_j - \kappa r_j}{1 + \kappa} = \frac{r_j - q_j}{1 + \kappa} = \frac{|q_j - r_j|}{1 + \kappa}.$$
(42)

• Case 2: Expansion  $(q_j > r_j)$ . We can derive that

$$|r_{j+1} - r_j| = r_{j+1} - r_j = \left(\frac{q_j - \kappa r_j}{1 - \kappa}\right) - r_j = \frac{q_j - \kappa r_j - r_j(1 - \kappa)}{1 - \kappa} = \frac{q_j - r_j}{1 - \kappa} = \frac{|q_j - r_j|}{1 - \kappa}.$$

Since  $\kappa < 1$  while being positive, we have  $1 - \kappa < 1 + \kappa$ . The denominator is smaller in the expansion case, so the worst-case bound for  $|r_{j+1} - r_j|$  is given as

$$|r_{j+1} - r_j| \le \frac{1}{1 - \kappa} |q_j - r_j|,$$
 (43)

which was to be proven. Finally, in the case that  $q_j < r_j$ , we see that the numerator in (42) is positive, and since  $1 + \kappa > 0$ , the change is positive, meaning  $r_{j+1} < r_j$ .

#### C.7 Proof of Theorem 3

Step 1: Setup and notation. For the convenience of the reader, we first recall our notation. Let

$$T(r) = Q_{1-\alpha}(\pi^{\star}(r))$$

denote the  $(1-\alpha)$  true population quantile under policy  $\pi^*(r)$ . We assume the Lipschitz property

$$|T(r) - T(r')| \le \kappa |r - r'|$$
 for all  $r, r' \in \mathbb{R}_{>0}$ ,

where  $\kappa = \beta_T L_U \in (0,1)$  is the closed-loop gain. Suppose there exists a fixed point  $r^* \in \mathbb{R}_{\geq 0}$  with

$$T(r^{\star}) = r^{\star}.$$

Let the episode-j error and calibration perturbation be

$$e_j = |r_j - r^*|, \qquad \eta_j = q_j - T(r_j),$$
 (44)

where  $q_j$  is the empirical  $(1 - \bar{\alpha}_j)$  quantile formed with

$$\bar{\alpha}_j = \alpha - \sqrt{\frac{\ln(1/\delta)}{2 n_j}} \in (0, \alpha).$$

Here  $\delta \in (0,1)$  is the level-tightening parameter appearing inside  $\bar{\alpha}_j$ ; see the main text. We will use a separate symbol  $\delta_j$  below for per-episode tail probabilities in high-probability bounds.

Step 2: Branch-wise identities induced by the explicit update. Write  $q_j = T(r_j) + \eta_j$  by (44). The explicit update from Theorem 3 gives us the following expressions:

if 
$$q_j \le r_j$$
 (shrinkage):  $(1+\kappa) (r_{j+1} - r^*) = (T(r_j) - T(r^*)) + \kappa (r_j - r^*) + \eta_j$ , (45)

if 
$$q_j > r_j$$
 (expansion):  $(1 - \kappa) \left( r_{j+1} - r^* \right) = \left( T(r_j) - T(r^*) \right) - \kappa \left( r_j - r^* \right) + \eta_j$ . (46)

*Derivation.* In the shrinkage case, in order to obtain (45), we compute  $r_{j+1} - r^*$  while substituting  $r_{j+1} = \frac{q_j + \kappa r_j}{1 + \kappa}$  and  $q_j = T(r_j) + \eta_j$  so that

$$(1+\kappa)(r_{j+1}-r^*) = q_j + \kappa r_j - (1+\kappa)r^* = T(r_j) - T(r^*) + \kappa(r_j - r^*) + \eta_j.$$

The expansion case is identical with  $r_{j+1} = \frac{q_j - \kappa r_j}{1 - \kappa}$ .

**Step 3: One-step bounds and contraction threshold.** Taking absolute values in (45)–(46) and using the Lipschitz property

$$|T(r_j) - T(r^*)| \leq \kappa |r_j - r^*| = \kappa e_j,$$

we obtain

$$|r_{j+1} - r^*| \le \frac{1}{1+\kappa} \Big( |T(r_j) - T(r^*)| + \kappa e_j + |\eta_j| \Big) \le \frac{2\kappa}{1+\kappa} e_j + \frac{1}{1+\kappa} |\eta_j|,$$

$$|r_{j+1} - r^*| \le \frac{1}{1-\kappa} \Big( |T(r_j) - T(r^*)| + \kappa e_j + |\eta_j| \Big) \le \frac{2\kappa}{1-\kappa} e_j + \frac{1}{1-\kappa} |\eta_j|.$$

The coefficients in the expansion case dominate those coefficients in the shrinkage case so for that for all

episodes j we obtain the one-step recursion

$$e_{j+1} \le \gamma_{\kappa} e_j + B_{\kappa} |\eta_j|, \qquad \gamma_{\kappa} = \frac{2\kappa}{1-\kappa}, \quad B_{\kappa} = \frac{1}{1-\kappa}.$$
 (47)

We specifically note that

$$\gamma_{\kappa} < 1 \iff \frac{2\kappa}{1-\kappa} < 1 \iff 3\kappa < 1 \iff \kappa < \frac{1}{3}.$$
 (48)

**Step 4: Explicit finite-horizon error bound.** We now unroll (47) over multiple episodes to obtain (16), which is the first result to be shown. For convenience, we recall (16) as

$$e_{j+1} \le \gamma_{\kappa}^{j+1} e_0 + B_{\kappa} \sum_{m=0}^{j} \gamma_{\kappa}^{j-m} |\eta_m|.$$
 (49)

Base case j=0. From (47),  $e_1 \le \gamma_{\kappa} e_0 + B_{\kappa} |\eta_0|$ , which matches (49) with j=0. Induction step. Assume (49) holds for some  $j \ge 0$ . Then

$$e_{j+2} \leq \gamma_{\kappa} e_{j+1} + B_{\kappa} |\eta_{j+1}| \leq \gamma_{\kappa} \left( \gamma_{\kappa}^{j+1} e_0 + B_{\kappa} \sum_{m=0}^{j} \gamma_{\kappa}^{j-m} |\eta_m| \right) + B_{\kappa} |\eta_{j+1}|,$$

which simplifies to

$$e_{j+2} \leq \gamma_{\kappa}^{j+2} e_0 + B_{\kappa} \sum_{m=0}^{j+1} \gamma_{\kappa}^{j+1-m} |\eta_m|,$$

i.e., (49) with  $j \leftarrow j + 1$ . This completes the induction.

Step 5: Closed-form bounds. If  $|\eta_m| \le C$  for all  $m \in \{0, 1, \dots, j\}$ , then applying (49) and summing the geometric series gives

$$e_{j+1} \leq \gamma_{\kappa}^{j+1} e_0 + B_{\kappa} C \sum_{m=0}^{j} \gamma_{\kappa}^{j-m} = \gamma_{\kappa}^{j+1} e_0 + B_{\kappa} C \sum_{\ell=0}^{j} \gamma_{\kappa}^{\ell}$$
$$= \gamma_{\kappa}^{j+1} e_0 + B_{\kappa} C \frac{1 - \gamma_{\kappa}^{j+1}}{1 - \gamma_{\kappa}}.$$
 (50)

If moreover  $\kappa < \frac{1}{3}$  (so that  $\gamma_{\kappa} < 1$ ), then letting  $j \to \infty$  in (50) yields the steady-state bound

$$\limsup_{j \to \infty} e_j \le \frac{B_{\kappa}}{1 - \gamma_{\kappa}} C = \frac{1}{1 - 3\kappa} C.$$

This proves the second result of Theorem C.7 in equation (17).

#### Step 6: High-probability control of $\eta_i$ (level shift + empirical error). First, decompose

$$\eta_{j} = \underbrace{Q_{1-\bar{\alpha}_{j}}(\pi^{\star}(r_{j})) - Q_{1-\alpha}(\pi^{\star}(r_{j}))}_{\Delta_{j}^{\text{lvl}}} + \underbrace{q_{j} - Q_{1-\bar{\alpha}_{j}}(\pi^{\star}(r_{j}))}_{\varepsilon_{j}^{\text{est}}}$$

into a level shift and empirical error component.

By assumption, the CDF  $F_{r_j}(s)$  is differentiable and has density no less than  $f_{\star}>0$  in a sufficiently large neighborhood of its  $(1-\alpha)$  quantile  $Q_{1-\alpha}(\pi^{\star}(r_j))$ . Then, by Lemma 4 which we separately present in Appendix C.8, the inverse-CDF is  $1/f_{\star}$ -Lipschitz in the probability level, and therefore

$$\left|\Delta_{j}^{\text{lvl}}\right| \leq \frac{\left|\alpha - \bar{\alpha}_{j}\right|}{f_{\star}}.\tag{51}$$

Next, Lemma 5 which we separately present in Appendix C.8 and the inverse-CDF Lipschitz property imply

$$\mathbb{P}_{n_j} \left\{ \left| \varepsilon_j^{\text{est}} \right| \le \frac{1}{f_{\star}} \sqrt{\frac{\ln(2/\delta_j)}{2n_j}} \right\} \ge 1 - \delta_j. \tag{52}$$

where  $\delta_j \in (0,1)$  is any prescribed failure probability.

Combining (51)–(52) gives the per-episode high-probability bound

$$\mathbb{P}_{n_j} \left\{ |\eta_j| \le \frac{|\alpha - \bar{\alpha}_j|}{f_\star} + \frac{1}{f_\star} \sqrt{\frac{\ln(2/\delta_j)}{2n_j}} \right\} \ge 1 - \delta_j, \tag{53}$$

which proves equation (18) in Theorem 3.

Finally, applying equation (49) and a union bounding argument over the first j+1 episodes, we obtain the explicit finite-horizon control

$$\mathbb{P}_{\sum_{m=0}^{j} n_{m}} \left\{ e_{j+1} \leq \gamma_{\kappa}^{j+1} e_{0} + \frac{B_{\kappa}}{f_{\star}} \sum_{m=0}^{j} \gamma_{\kappa}^{j-m} |\alpha - \bar{\alpha}_{m}| + \frac{B_{\kappa}}{f_{\star}} \sum_{m=0}^{j} \gamma_{\kappa}^{j-m} \sqrt{\frac{\ln(2/\delta_{m})}{2n_{m}}} \right\} \geq 1 - \sum_{m=0}^{j} \delta_{m}.$$

This shows equation (19) in Theorem 3. Here the sequence  $\{\delta_m\}$  is independent of the level-tightening parameter  $\delta$  used in  $\bar{\alpha}_m$ ; the former controls empirical quantile fluctuations, the latter sets the calibration level.

Step 7: Asymptotic conclusions. If  $n_j \to \infty$  and  $\bar{\alpha}_j \to \alpha$ , then both terms in (53) vanish and  $|\eta_j| \to 0$ . If  $\kappa < \frac{1}{3}$ , then  $\gamma_{\kappa} < 1$  by (48) and (49) gives  $e_j \to 0$ . If further  $\bar{\alpha}_j \equiv \bar{\alpha} < \alpha$  and  $n_j \to \infty$ , then  $|\eta_j| \to (\alpha - \bar{\alpha})/f_{\star}$ . Using (50) with  $C = (\alpha - \bar{\alpha})/f_{\star}$  yields

$$\limsup_{j \to \infty} e_j \leq \frac{1}{1 - 3\kappa} \cdot \frac{\alpha - \bar{\alpha}}{f_{\star}}.$$

This completes the proof of Theorem 3.

#### C.8 Quantile perturbation lemmas (expanded and annotated)

**Setup and notation.** Recall that  $F_r: \mathbb{R} \to [0,1]$  denotes the cumulative distribution function (CDF) of the nonconformity score  $s(\hat{y}_{0:T}, Y_{0:T})$  for the trajectory  $y_{0:T} \sim \mathcal{D}(\pi^*(r))$ . We have also defined the right-continuous quantile map as

$$Q_p(\pi^*(r)) := \inf\{s \in \mathbb{R} : F_r(s) \ge p\}, \qquad \alpha \in (0,1).$$

Assume that the CDF  $F_r(s)$  is differentiable and has density  $f_r(s)$  no less than  $f_{\star} > 0$  for all s in a sufficiently large neighborhood of its p quantile  $Q_p(\pi^{\star}(r))$ , i.e.,

$$f_r(s) \ge f_\star > 0$$
 for all  $s$  in a sufficiently large neighborhood of  $Q_p(\pi^\star(r))$ . (54)

Condition (54) guarantees that the inverse-CDF is locally Lipschitz; geometrically, the CDF has a slope bounded away from 0 near the quantile, so small changes in probability level produce controlled changes in the quantile value.

**Lemma 4** (Level-to-quantile Lipschitzness). For any two probability levels  $p, p' \in (0, 1)$  and for any  $Q_{p'}(\pi^*(r))$  in the neighborhood of  $Q_p(\pi^*(r))$  from (54), we have that

$$|Q_p(\pi^*(r)) - Q_{p'}(\pi^*(r))| \le \frac{|p - p'|}{f_+}.$$
 (55)

*Proof.* 1) Fix the two quantiles. Let

$$q = Q_p(\pi^*(r)), \qquad q' = Q_{p'}(\pi^*(r)).$$

By definition of  $Q_p$ , we have  $F_r(q) \ge p$  and, by right continuity and strict monotonicity in our neighborhood, we can take  $F_r(q) = p$  and  $F_r(q') = p'$ .

2) Apply the Mean Value Theorem (MVT). Since  $F_r$  is differentiable on the open interval between q and q', there exists a point  $\xi$  between q and q' such that

$$F_r(q') - F_r(q) = f_r(\xi) (q' - q).$$

3) Use the density lower bound. Because  $f_r(\xi) \geq f_{\star}$  by (54), we get

$$|p'-p| = |F_r(q') - F_r(q)| = f_r(\xi)|q'-q| \ge f_{\star}|q'-q|.$$

4) Rearrange. Hence

$$|q'-q| \le \frac{|p'-p|}{f_{\star}},$$

which is (55).

Why we need Lemma 4. In the convergence analysis (Theorem 3), we compare the population quantiles at two *levels*,  $1 - \bar{\alpha}_i$  (used for calibration) and  $1 - \alpha$  (the target). Lemma 4 gives the clean bound

$$|Q_{1-\bar{\alpha}_j} - Q_{1-\alpha}| \le \frac{|\alpha - \bar{\alpha}_j|}{f_{\star}},$$

which is the level-shift term in the perturbation  $\eta_j$ .

**Lemma 5** (Empirical quantile error via DKW Inequality). Let  $F_{r,n}$  be the empirical CDF from n i.i.d. samples drawn from  $F_r$ , and let  $q_{n,p}$  be the empirical p-quantile  $q_{n,p} = \inf\{t : F_{r,n}(t) \ge p\}$ . Then, for any outer tail level  $\delta \in (0,1)$ , we have

$$\mathbb{P}_n \left\{ \sup_{t \in \mathbb{R}} \left| F_{r,n}(t) - F_r(t) \right| \le \varepsilon_n(\delta) \right\} \ge 1 - \delta, \qquad \varepsilon_n(\delta) := \sqrt{\frac{\ln(2/\delta)}{2n}}. \tag{56}$$

Under the assumption in equation (54), the empirical quantile satisfies

$$\mathbb{P}_n \left\{ \left| q_{n,p} - Q_p(\pi^*(r)) \right| \le \frac{\varepsilon_n(\delta)}{f_\star} \right\} \ge 1 - \delta.$$
 (57)

*Proof.* 1) DKW event (uniform CDF control). By the DKW inequality, the statement in equation (56) immediately follows.

2) Pin the target quantile and a local window. Let

$$q^{\star} = Q_{p}(\pi^{\star}(r)),$$

and pick a small  $\Delta > 0$  that keeps  $[q^* - \Delta, q^* + \Delta]$  inside the neighborhood where  $f_r \geq f_*$ .

3) One-sided controls for the *true* CDF using the density lower bound. By the Mean Value Theorem applied to  $F_r$  on  $[q^*, q^* + \Delta]$  and  $[q^* - \Delta, q^*]$  there exist points  $\xi_+, \xi_-$  in those intervals with

$$F_r(q^* + \Delta) - F_r(q^*) = f_r(\xi_+) \Delta \ge f_*\Delta, \qquad F_r(q^*) - F_r(q^* - \Delta) = f_r(\xi_-) \Delta \ge f_*\Delta.$$

Since  $F_r(q^*) = p$ , we get

$$F_r(q^* + \Delta) \ge p + f_*\Delta, \qquad F_r(q^* - \Delta) \le p - f_*\Delta.$$
 (58)

4) Transfer these inequalities to the *empirical CDF* on the DKW event. Using (56), we have

$$\mathbb{P}_n\{F_{r,n}(q^* + \Delta) > F_r(q^* + \Delta) - \varepsilon > p + f_*\Delta - \varepsilon \tag{59}$$

and 
$$F_{r,n}(q^* - \Delta) \le F_r(q^* - \Delta) + \varepsilon \le p - f_*\Delta + \varepsilon \ge 1 - \delta.$$
 (60)

5) Choose  $\Delta$  to make the inequalities straddle level p. Set  $\Delta = \frac{\varepsilon}{f_+}$  so that

$$\mathbb{P}_n\{F_{r,n}(q^* + \Delta) \geq p \text{ and } F_{r,n}(q^* - \Delta) \leq p\} \geq 1 - \delta.$$

6) Use the empirical quantile definition to trap  $q_{n,p}$ . By definition,  $q_{n,p}=\inf\{t: F_{r,n}(t)\geq p\}$ . Since  $F_{r,n}(q^\star-\Delta)\leq p$  and  $F_{r,n}(q^\star+\Delta)\geq p$ , the monotonicity of  $F_{r,n}$  implies

$$\mathbb{P}_n\{q_{n,p} \in [q^* - \Delta, q^* + \Delta]\} \ge 1 - \delta,$$

where we used the union bound. Therefore,

$$\mathbb{P}_n\bigg\{|q_{n,p}-q^\star| \leq \Delta = \frac{\varepsilon}{f_\star} = \frac{\varepsilon_n(\delta)}{f_\star}\bigg\} \geq 1-\delta.$$

This is exactly (57).

Why we need Lemma 5. In the convergence proof, the empirical quantile  $q_j$  is compared to the population quantile at the *same level*  $1 - \bar{\alpha}_j$ . Lemma 5 converts the uniform CDF error (obtained using the DKW inequality) into an error on the quantile value, with the sharp factor  $1/f_{\star}$ . Concretely, we thereby get

$$\mathbb{P}_{n_{j}} \left\{ \left| q_{j} - Q_{1-\bar{\alpha}_{j}}(\pi^{\star}(r_{j})) \right| \leq \frac{1}{f_{\star}} \sqrt{\frac{\ln(2/\delta_{j})}{2 n_{j}}} \right\} \geq 1 - \delta_{j}.$$